Modeling local and cross-species neuron number variations in the cerebral cortex as arising from a common mechanism

Diarmuid J. Cahalane[a], Christine J. Charvet[b], and Barbara L. Finlay[b,1]

[a]Center for Applied Mathematics and [b]Department of Psychology, Cornell University, Ithaca, NY 14853

Edited by Pasko Rakic, Yale University, New Haven, CT, and approved October 15, 2014 (received for review June 6, 2014)

A massive increase in the number of neurons in the cerebral cortex, driving its size to increase by five orders of magnitude, is a key feature of mammalian evolution. Not only are there systematic variations in cerebral cortical architecture across species, but also across spatial axes within a given cortex. In this article we present a computational model that accounts for both types of variation as arising from the same developmental mechanism. The model employs empirically measured parameters from over a dozen species to demonstrate that changes to the kinetics of neurogenesis (the cell-cycle rate, the progenitor death rate, and the "quit rate," i.e., the ratio of terminal cell divisions) are sufficient to explain the great diversity in the number of cortical neurons across mammals. Moreover, spatiotemporal gradients in those same parameters in the embryonic cortex can account for cortex-wide, graded variations in the mature neural architecture. Consistent with emerging anatomical data in several species, the model predicts (*i*) a greater complement of neurons per cortical column in the later-developing, posterior regions of intermediate and large cortices, (*ii*) that the extent of variation across a cortex increases with cortex size, reaching fivefold or greater in primates, and (*iii*) that when the number of neurons per cortical column increases, whether across species or within a given cortex, it is the later-developing superficial layers of the cortex which accommodate those additional neurons. We posit that these graded features of the cortex have computational and functional significance, and so must be subject to evolutionary selection.

cerebral cortex | evolution | development | neurogenesis | mathematical modeling

Changes in brain structure follow a remarkably stable pattern over ~450 My in the vertebrate lineage: it is always the same brain parts that become enlarged when overall brain size increases (1). Moreover, in studies of individual variation in humans and other mammals, when overall brain size is larger, those same divisions as would be predicted by looking at brain enlargement across taxa are also found to be preferentially enlarged (2, 3). Such regularities in brain scaling from the individual to the taxon level suggest that the developmental mechanisms which generate central nervous systems are strongly conserved across species (4).

To tease apart the features of the isocortex contributed by the scaling of conserved developmental mechanisms from those features which might be specially selected for in a given niche or species, we have created an empirically informed, mathematical model of cortical neurogenesis. The model elucidates how the dials and levers made available by conserved developmental mechanisms allow selection to shape the basic landscape of the embryonic cortex. The extent to which any particular cortical area (e.g., a visual or language area) has been a special subject of selection can be better evaluated given the baselines provided by this evolutionary developmental or "evo-devo" model.

The modeling approach presented here provides an explicit structure to assimilate known data and predict unknowns, both for developmental kinetic parameters and for the resultant time courses of neuronal and progenitor cell populations, for the entire range of mammalian brain sizes and across a spatial axis within the respective cortices. Our model incorporates important insights from several previously published mathematical models of cortical neurogenesis which focus on more limited sets of species or which consider spatial variations in a single species (5–10).

Scope of the Model

The mathematical model aims to mimic a set of key, basic processes by which cortical neurons are produced and distributed to cortical layers. Here we summarize those processes and also point out other sources of cortical structure which are not within the scope of the model.

Key Features of Cortical Neurogenesis. A founding population of precursor cells in ventricular zones near the wall of the cerebral vesicles initially undergoes rounds of symmetric division, whereby both daughter cells are precursors, thus swelling the precursor pool. Neurogenesis begins when some divisions in the precursor pool become asymmetric: with some probability a daughter cell is now a differentiated neuron which will not undergo further rounds of cell division and will migrate out of the ventricular zone (5, 11). Our dynamical model tracks the size of two populations: the precursor pool and its neuronal progeny. After Caviness and coworkers, we refer to the probability of a daughter cell being a neuron as the "quit fraction" (5). As neurogenesis proceeds, the quit fraction becomes larger [although variations from monotonic increase have been reported (12) and are tested in the present model]. When the quit fraction

Significance

Despite great diversity across mammals in the number of cortical neurons and the cognitive functions they support, the fundamental process which populates the cerebral cortex with neurons changes only subtly from the smallest rodents to the largest primates. Understanding how the dynamics of neurogenesis can vary will help unravel how the genome molds normal and disrupted cortical development. We gathered data on the growing and mature cortex to build a computational model of neurogenesis. The model recapitulates how dynamics, known to vary across species and across the cortex, sculpt the basic landscape of the embryonic cortex. Features of the cortex long thought to be the result of special selection are revealed as the necessary product of a conserved mechanism.

Author contributions: D.J.C. and B.L.F. designed research; D.J.C. and C.J.C. performed research; D.J.C. contributed new reagents/analytic tools; D.J.C. and C.J.C. analyzed data; and D.J.C. and B.L.F. wrote the paper.

The authors declare no conflict of interest.

This article is a PNAS Direct Submission.

[1]To whom correspondence should be addressed. Email: blf2@cornell.edu.

This article contains supporting information online at www.pnas.org/lookup/suppl/doi:10.1073/pnas.1409271111/-/DCSupplemental.

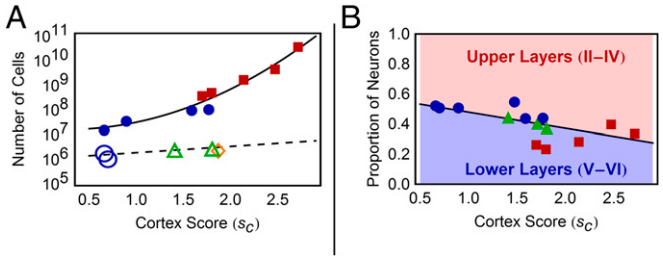

Fig. 1. (*A*) Estimates for the founder population (dashed line) and total neuronal output of the ventricular zone (solid line) as a function of cortex score s_c. The solid symbols represent adult cortical neuron counts in rodents (blue disks) and primates (red squares), each multiplied by a factor of 1.5 to allow for the large fraction of neurons that dies after reaching the cortex. The open symbols represent empirical counts of cells in the precursor pools of rodents (blue circles), carnivores (green triangles), and a sheep (orange diamond). The ratio of the two fitted functions gives an estimate of the amplification factor for a given cortex score. See *SI Appendix*, Tables S1 and S2 for data and sources. (*B*) To estimate the proportion of neurons whose adult location is in the upper layers (II–IV) versus lower layers (V and VI) of the cortex, a linear regression of the proportion as assessed in six rodents (blue disks), three carnivores (green triangles), and five primates (red squares) against cortex score s_c is carried out. For species and sources, see *SI Appendix*, Table S3.

is greater than one-half, the majority of the cells produced are neurons and the precursor pool depletes. Along with the quit fraction, the model includes two other time-dependent kinetic parameters: the cell-cycle duration and the probability that either of the two cells resulting from a division dies. Neurons migrate to populate the developing layers of the cortex, the first produced neurons being more likely to populate the deep cortical layers (VI and V); neurons destined for the progressively more superficial layers (VI through II) subsequently migrate through the already-present layers (8, 13, 14). In our model, the relative probability of a neuron being assigned to an upper or lower cortical layer varies dependent on its time of production.

Our model does not incorporate other factors which cause local, area-dependent variations in neuron number during neurogenesis and later in development, for example, incident axonal projections of the various sensory modalities entering the cortex at particular locations or locally present genetic cues (15–17). In *Discussion*, we consider how such sources of variation can add richer structure to the smoothly changing cortical landscape produced by our model.

Empirical Support. Necessary empirical data to inform the model's inputs and to test its predictions against measured numbers of neurons, postnatally or in adulthood, are distributed with varying degrees of completeness over 6–10 mammalian species. These data include the number of precursor cells, the adult distribution of cortical neurons, the developmental timing of cortical neurogenesis, and kinetic parameters (cell-cycle rates, death rates, and the quit fraction). From this information we estimate targets for precursor amplification and adult layer distribution of neurons across the range of mammalian brain sizes from small rodents to primates (Fig. 1) (18–24). For the kinetic parameters governing the cell-cycle rate and the quit rate (but not for the death rate, for which we used fixed parameters), we used published data to inform initial guesses of these parameters (5, 13, 14, 25–29) and then, for each cortex size, we searched over many candidate sets of the parameters to find those producing the best match to the targets for amplification and layer assignment of neurons.

Results

The model presented in this article can account for the massive increase over mammalian evolution in the number of cortical neurons as arising from biologically plausible, continuous changes to the kinetic parameters of a developmental mechanism which is conserved across species (Fig. 2). The initial cortical precursor population is not required to change significantly across species to support the change of approximately five orders of magnitude in the size of the adult cortical neuronal population. The increase in total adult number of cortical neurons is predicted to have a concomitant increase in the proportion of those neurons occupying the upper layers (II–IV) of the cerebral cortex. The model explains recently demonstrated global gradients (reaching up to fivefold variation, but also subject to local, areal deviations) in the number of neurons per column across a spatial axis in primate cortices (30, 31) as arising from intracortical gradients in the kinetics of neurogenesis which are known to exist in rodents, carnivores, and primates (13, 27, 32–36). A reduced gradient observed in a number of rodents is also consistent with the model's predictions (Fig. 3) (20). In all cases, the model predicts a gradient

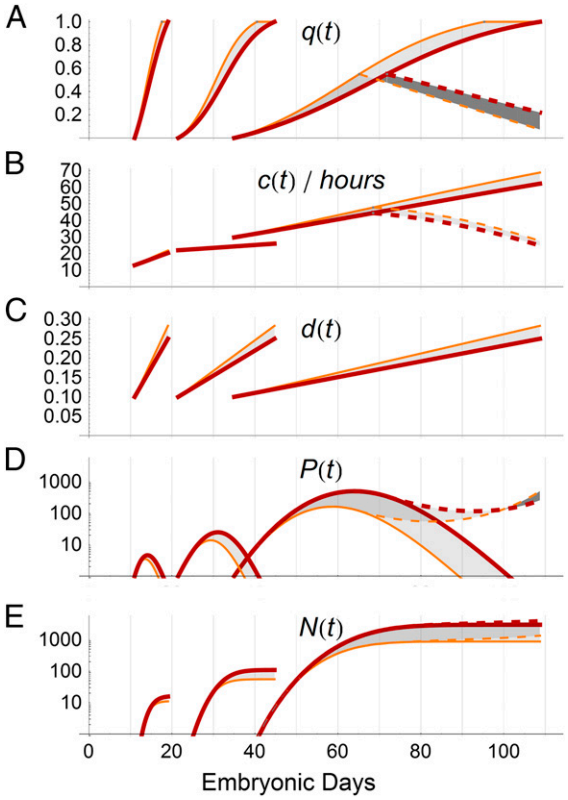

Fig. 2. Model neuronal output over embryonic days, across the cortex for mouse (*Left*) cortex score 0.701, ferret (*Middle*) cortex score 1.714, and macaque (*Right*) cortex score 2.472. Model parameters for (*A*) the quit fraction, (*B*) the cell-cycle duration in hours, and (*C*) the death rate in the ventricular zone result in trajectories for the precursor pool (*D*) and the total neuronal population (*E*) given on a log scale as a multiple of the initial precursor populations for each species. The thick red line in each case corresponds to the later-developing (typically posterior) regions, compared with the earlier progressing (typically anterior) cortex, represented by the thinner yellow line. The cross-cortex gradient in neuronal output is predicted to be more pronounced in those species with a larger cortex. An alternative set of parameters, represented by dashed lines in *A* and *B*, is tested for macaque only; the resultant populations are given by the dashed lines in *D* and *E*. Empirical evidence suggests a nonmonotonic trajectory for $q(t)$ and $c(t)$ in macaque, although the persistence of a large precursor pool in late neurogenesis, as implied by the present model, is not expected; see *Discussion*.

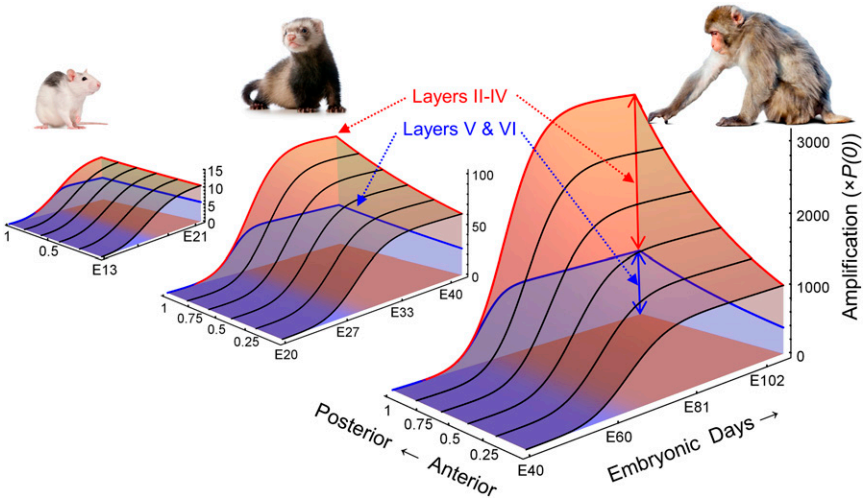

Fig. 3. Model-predicted interspecies and intracortex differences in the timing, extent, and layer assignment of cortical neuron output. Shown here are the predicted amounts of neuronal output (in terms of amplification of a unit precursor pool) across the anterior–posterior (spatial) axis of the cortex over the course of embryonic neurogenesis (time axis) for three different cortex scores (1.0, similar to a rat; 1.75, similar to a ferret; 2.5, similar to a macaque monkey). The larger cortices have a longer developmental interval, produce orders of magnitude more neurons in total and, in particular, have a greater complement of upper layer neurons. The anterior–posterior gradient in neuron number becomes more pronounced in larger cortices and it is the upper layers which accommodate the greater proportion of the increasing quantities of neurons. Rat and ferret images courtesy of iStockphoto/GlobalP. Macaque image courtesy of iStockphoto/JackF.

in total neuron number and the ratio of infra- to supragranular layer neurons along a spatial axis.

Cross-Species Increases in Neuron Number and Upper Layer Proportion. We have identified coordinate changes to the progression of the quit fraction $q(t)$, the cell-cycle duration $c(t)$, and the cell death rate $d(t)$ which can account, to high accuracy, for the changes seen in upper and lower cortical neuron numbers across the range of mammalian cortex sizes. The accuracy with which the empirical targets for those neuron numbers are reproduced is within 4% of the target values in all cases and within less than 1% for intermediate and larger cortices (*SI Appendix*, Fig. S7*F*). Our search scheme does not exhaust the space of biologically plausible parameters, so it may be assumed that higher accuracy is possible. However, the current absence of empirical data with which to compare such predictions, along with the approximate nature of the targets, means the pursuit of higher accuracy predictions is of uncertain value at this time. For example, future anatomical data may support the suggestion that the layer proportion of neurons varies by taxonomic group and not only by cortex size. In that eventuality, the model's targets ought to also reflect group differences in upper and lower neuron number, and this would necessarily change the best fit parameters for the species in question.

Studies have shown evidence that the cell-cycle rate (in ferret and monkey) and quit fraction (in monkey) may be reduced in late neurogenesis (12, 27, 28). We used the present model to predict the impact of such nonmonotonic parameter functions for $c(t)$ and $q(t)$ in the macaque (Fig. 2, dashed lines). Under our assumptions, the impact was to increase neuronal output modestly (by about an order of magnitude less than the change due to cross-cortical gradients) and there was the problematic prediction of a large precursor pool persisting as neurogenesis came to an end. The precise trajectory of kinetic parameters can be decisive, however, and future empirical measurements may resolve the discrepancy or reveal the model assumptions as being inadequate.

Intracortex Increases in Neuron Number and Upper Layer Proportion. Neurogenesis is known to progress at location-dependent rates, varying within the embryonic cortices of rodents, carnivores, and primates (13, 27, 32–36), whereby the nonlimbic isocortex is populated with neurons in a generally anterior to posterior progression. Modeling the effect of such spatial gradients in developmental timing (by adjusting the progression of the parameters in neurogenesis, as described in *Methods Summary*), the predicted outcome is a gradient in the number of neurons per column along the axis of variation. The extent of the gradient in neuron number, reaching up to fivefold in large primate cortices, is consistent with known anatomical gradients in primate neuron number (30, 31). The model predicts an accompanying shift in the layer proportion of neurons, favoring upper layers in the later-developing posterior cortex. Stereological measurements of upper and lower neuron numbers confirm that the increased complement of neurons per column in the posterior cortex of primates is largely contained in the upper layers; the absolute numbers of neurons per column in layers V and VI vary relatively little across the cortex (20). Existing models demonstrated that adjustments of the quit fraction have pronounced influence on total neuronal output (6, 7). Our model recapitulates that in the context of within-cortex variation (for an intermediate-sized cortex, with cortex score of 2.25, delaying the rise of the quit fraction by 30% gives a fourfold boost to neuronal output) and moreover predicts a concomitant shift in the ratio of upper to lower layer neurons.

Cross-Species Differences in the Extent of Intracortical Variation. Across species, the model predicts that larger cortices will have a far more pronounced gradient in neuron number and layer proportion: varying by fivefold in large primates and by just a few percent in small rodents. The longer period of gestation in primates makes the difference in neurogenesis end dates more notable in those species than in rodents. In the macaque monkey, despite beginning at approximately the same developmental time in all regions, neurogenesis ends as many as 3 wk later in posterior cortex—an intracortex difference of more than 30% in the length of the interval (35). By comparison, the anterior–posterior timing difference in rat may be as long as 2 d, amounting to perhaps a 25% intracortex difference in the duration of neurogenesis (13). Hence, the fractional differences in neurogenesis duration across species are not dissimilar. The impact of lengthening the period of neurogenesis by a given percentage depends, however, on how many additional rounds of cell division that extension will allow. Hence, larger brains, where many more of rounds of cell division take place during neurogenesis, will realize a disproportionate boost in neuronal output in those regions with extended neurogenesis. This leaves open the possibility that the intermediate-sized brains (of, e.g., ungulates and some carnivores) exhibit a gradient of intermediate slope.

Discussion

Limitations of the Current Model. We have outlined a basic model in which the kinetics of neurogenesis give rise to an embryonic cortex whose architecture varies smoothly and systematically along a spatial axis. However, variations in the mature distribution of cortical neurons are not so smooth, exhibiting local

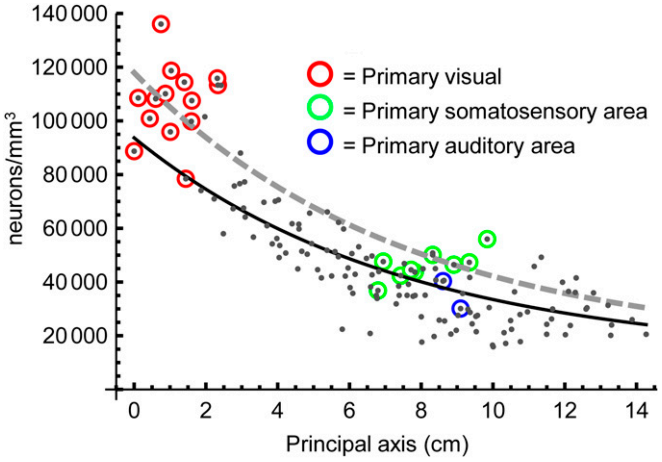

Fig. 4. Using a two-factor model (location and an indicator for primary or nonprimary area) of neuronal density is better than a location-only model. In the two-factor model, primary sensory areas have a neuronal density 26% higher than would a nonprimary sensory area at the same location (the dashed line is 1.26× the base level density indicated by the solid line). The origin of the spatial "principal" axis is at the posterior medial pole of the flattened cortex and it extends toward the anterior lateral pole.

deviations in density such as an abrupt change across the boundary of visual areas 1 and 2, and higher density in sensory processing areas than adjacent areas (31). We conjecture that the smooth gradients establish the basic landscape that richer areal and cellular structure is built upon, as prompted by genetic markers, projections from subcortical structures, or other locally present cues (15–17). We offer the following as an example of how local deviations could be overlaid on the basic landscape set up by the global gradient in neuron number.

Collins et al. noted that areas involved in sensory processing had higher neuron densities than some adjacent areas (31). In our previously published reanalysis of the data of Collins et al., we identified the data points which relate to primary sensory areas in baboon and we used a two-factor statistical model to look for significant differences in the neuronal density of sensory areas from what a "location-only" model predicted (30). We found that primary areas have a density of neurons which is 26% higher than that predicted for a nonprimary area in the same location along the global density gradient (Fig. 4). So, clearly, a mechanism other than smooth, global changes in neurogenesis is required to fully explain the variations in neuron density. As to potential mechanisms producing such local variations not included in the present model, lower levels of neuron death during early development have been reported in developing sensory areas relative to other areas (37) as well as local regulation of the cell cycle (16). We suggest that those mechanisms, acting in addition to the global gradients in neurogenesis output described above, and possibly in concert with further local mechanisms, may explain the greater number of neurons per unit column in primary sensory regions.

The present study also makes assumptions based on limited empirical data about the trajectories of the kinetic parameters and how such trajectories change across species and orders. In particular, we have assumed smooth change in kinetic parameters across cortex sizes whereas the reality may be that particular taxa exhibit idiosyncratic variations (12, 27, 28). Incorporating future empirical data to refine these assumptions and comparing the resultant model output to mature distributions of neurons will illuminate whether the processes included in the model are adequate or need to be augmented.

Furthermore, the parameter sets which can reproduce target neuron numbers for a given cortex score to high accuracy are not unique, as compensating changes to the various parameters can result in similar neuronal output (*SI Appendix*, Fig. S7). Future empirical observations will help to constrain the search space, revealing some parameter sets as implausible and thus refining the model's predictions concerning those parameters which remain unobserved. In addition to this, our model considers parameter variation along a single axis but additional axes of variation may exist in a given cortex.

Structural and Functional Implications. The generally anterior-to-posterior changes in cortical neuron number imply a corresponding variation in the types of neural processing that the respective regions of the cortex are most apt to support. In fact, the cortical variations we have highlighted are aligned with important functional and processing axes: higher stages of information processing and integration occur at progressively anterior locations in the cortex. For example, higher visual areas and association areas integrating visual information are in regions anterior to the primary visual areas (38). From somatosensory areas, information flows in the anterior direction to the motor areas where it informs motor control. The notion that anterior regions have more integrative roles in neural processing is also supported by their structural network connectivity: Modha and Singh found that regions in prefrontal cortex are distinguished by high network-topological centrality (39); studies finding a dense core within the cortical communications network identify nodes distributed across frontoparietal regions and elsewhere but not in the most neuron-dense occipital lobe (40, 41). We speculate that successively higher and more integrative stages of neural processing might be best supported by the less neuron-dense architecture bestowed on anterior cortex by developmental gradients. Thus, the developmental mechanisms which lead to within-cortex variations in neural architecture impact cortical function and so are presumably a target of selection.

Questions Arising. We have given a model of cortical neurogenesis which demonstrates how a conserved mechanism can explain both cross-species scaling and key within-cortex variations. What further empirical data may soon be available to support or challenge the degree to which coordinate changes, arising from conserved mechanisms, account for the structure of the cortex? And, in the midst of so much conservation, what remains variable and available to selection?

Regarding empirical data, cross-cortex isotropic fractionator studies in primates revealed the pronounced gradients in neuron number discussed above (31). Stereological measurements of neuron number carried out in this laboratory show a much more uniform distribution of neurons across the rodent cortex (20). Studies systematically sampling multiple sites in the cortices of nonprimates would help answer the question of whether gradients in neuron number and neuron layer assignment are an obligatory feature of an enlarged cortex or whether they are unique to primates.

As to what parameters remain accessible to selection, given highly conserved developmental mechanisms, we offer the following as a possible example. Even if neuron number were constrained to vary smoothly, in a graded manner, across the cortex, then the slope of that gradient might be subject to selection. It seems apparent that those smaller cortices produced by relatively few rounds of cell division have a limited scope to develop gradients in neuron number by way of spatial variation of neurogenesis. It is less clear, however, if or why large cortices could not be more or less varied across their spatial extent. Can the slope of the gradient be set independent of cortex size? Answering questions such as these will further the understanding of the cellular and molecular mechanisms at work in constructing the brain and of how those mechanisms are encoded in the genome.

Methods Summary

The following is an abridged description of the methods used; a more extensive description is given in *SI Appendix*.

Modeling the Neuronal Output of the Ventricular Zone. A system of two ordinary differential equations (ODEs) models the dynamics of precursor cell replication and neuron production in the ventricular zone. Denoting the number of precursor cells present at time t by $P(t)$ and the number of differentiated neurons present by $N(t)$, the following differential equations prescribe how those populations change in time during neurogenesis:

$$\frac{dP(t)}{dt} = P(t)\frac{\ln(2)}{c(t)}[1 - 2d(t) - 2q(t)(1 - d(t))]$$

$$\frac{dN(t)}{dt} = P(t)\frac{\ln(2)}{c(t)}[2q(t)(1 - d(t))],$$

where $c(t)$ is the cell-cycle duration, $d(t)$ is the independent probability that each daughter cell dies after a cell division, and $q(t)$ is the probability that a daughter cell is a differentiated neuron which quits the precursor pool and does not undergo further rounds of cell division. To interpret the equations, note that if d and q were equal to zero, the precursor pool would undergo exponential growth, doubling with each cell cycle of duration $c(t)$. It is the nondead quitting cells which swell the neuronal population and hence the rightmost quantity subtracted from the equation for precursors appears as the positive contribution to the neuronal population. As no neurons are present at the start of neurogenesis, $N(0) = 0$. The amplification factor achieved by the model is given by the ratio of $N(t)$ at $t = 1$ to the size of the initial precursor population.

The Cortex Score and a Universal Time Axis for Neurogenesis. The timing of neurodevelopmental events can be predicted with high precision across mammals via the "translating time" model (4, 19). The particular mathematical form of that model scales early neurodevelopmental intervals across mammals in a linear fashion. In the present context, this allows us to shift and scale the neurogenetic interval of any mammal to lie between $t = 0$ and $t = 1$ on a universal time axis (*SI Appendix*, Fig. S1). Differences in the length of neurodevelopmental schedules across species are reflected in the translating time formalism by the "species scores" s_s—loosely speaking, this is a proxy for how much the interval is scaled. Those scores provide a convenient axis on which to line up brains, the larger brains generally having higher s_s due to their longer developmental interval. In the translating time model, a primate-cortex factor s_{pc} reflects the fact that cortical development in primates is delayed relative to other orders. As the present study focuses on the cortex, we coin the term "cortex score" and denote it as s_c. The cortex score is simply the species score in the case of nonprimates ($s_c = s_s$) and for primates $s_c = s_s + s_{pc}$. For those species where a species score was not available in the literature, we used adult brain weight as an ad hoc proxy to estimate the species score (*SI Appendix*).

Modeling the Layer Assignment of Cortical Neurons. Data from developmental cell-labeling studies in rat (13) and monkey (14) are used to parameterize a function which apportions the neuronal output of the ODE model either to lower (layers V and VI) or upper (layers II–IV). At a given time t in the neurogenetic interval for a cortex score of s_c, the fraction $u(t; s_c)$ of total neuronal output is routed to the upper layers, and $1 - u(t; s_c)$ to the lower layers, where $u(t; s_c)$ is a sigmoid-shaped function given by

$$u(t; s_c) = \frac{1}{2}\left(1 + \mathrm{erf}\left(\frac{t - t_{switch}(s_c)}{w}\right)\right).$$

The parameter t_{switch} determines the scaled time at which $u(t; s_c) = 0.5$, w determines the width of the sigmoid's cross-over, and erf is the Gauss error function (*SI Appendix*, Figs. S3 and S4 and section S3). For a given cortex score, empirical data support an estimate of $t_{switch}(s_c) = 0.675–0.114s_c$. The parameter w is fixed at 10.3% of length of the neurogenetic interval, as that is the mean value measured in both rat and monkey. We can interpret $u(t; s_c)$ as a probability at the level of individual neurons or as a fraction of instantaneous output at the population level.

Estimating the Required Amount of Neuronal Amplifications and the Target Adult Layer Distributions of Neurons Using Precursor Pool and Adult Data. Data from the literature on precursor pool sizes were collated alongside our laboratory's stereological measurements (*SI Appendix*, Table S1 and section S8). Data on the adult total neuron number were also collated (*SI Appendix*, Table S2). A substantive fraction of neurons dies after reaching the cortex (this is distinct in our model from cell death occurring in the ventricular zone), so the adult neuron population numbers are multiplied by a factor of 1.5 to estimate the total output of cortical neurogenesis (42, 43). Fig. 1*A* shows the precursor pool numbers and 1.5× the adult neuron numbers, along with functions that we fitted to estimate how the same change versus cortex score. Taking the ratio of the two fitting functions in Fig. 1*A*, we estimate the amplification factor a for a given cortex score to be $a(s_c) = \exp(2.81 - 1.254s_c + 1.256s_c^2)$.

Fig. 1*B* displays the regression line we fit to the available adult layer distribution data (*SI Appendix*, Table S3) versus cortex score. This lines serves as the target for neuronal layer proportion for a given species score (see *SI Appendix* for fit details).

Assimilating Empirical Data for Kinetic Parameters. Data from the literature are used to generate initial estimates of the parameters determining the shape of functions modeling the quit fraction $q(t)$, the cell-cycle duration $c(t)$, and the cell death rate $d(t)$ for each value of the cortex score (i.e., across the range of cortex sizes). Given the initial estimate for each parameter, a range of neighboring values is considered. The final choice of the parameter set for a given species is that which most closely reproduces the target population of neurons in the upper and lower layers, and depletes the precursor pool.

The progression of the quit fraction is modeled as a modified sigmoid $q(t;\alpha,\beta)$, constrained to have $q(0) = 0$ and $q(1) = 1$ (with the exception of the latter being relaxed for the test case for macaque shown in Fig. 2). The width of the sigmoid's cross-over is controlled by the parameter α and the midpoint of the cross-over is reached at time $t = \beta$ (see *SI Appendix*, section S5 for details). Initial estimates for α and β are based on empirical data for mouse from ref. 5 (*SI Appendix*, Fig. S5).

The cell-cycle duration, expressed as a fraction of each species' duration of neurogenesis, is modeled as $c(t) = c(t; \gamma, \delta) = \gamma + (\delta - \gamma)t$ (again with the exception of the test case for macaque shown in Fig. 2) Data from mouse, rat, ferret, and macaque provide initial estimates for γ and δ as a function of cortex score (25–29) (*SI Appendix*, section S5).

The progression of the cell death rate is modeled as $d(t) = d(t; \varepsilon, \phi) = \varepsilon + \phi t$. Data from rat (44) inform the estimates $\varepsilon = 0.1$ (the value at $t = 0$) and $\phi = 0.15$ [resulting in $d(1) = 0.25$], and it is assumed, in the absence of other data, that these values apply across the range of cortex scores. In contrast with the other kinetic functions, and to make sure the search is sufficiently constrained, the parameters for cell death above are assumed and are not optimized by the parameter search.

The parameter τ relates to the layer assignment function, $u(t; s_c)$. The parameter fitting algorithm can shift $u(t; s_c)$ along the time by an amount τ, to amend misalignments between the empirically informed $u(t; s_c)$ and the model's time axis.

Finding the Best Fit for Kinetic Parameters. For a given candidate set of parameter values $m_i = \{\alpha_i, \beta_i, \gamma_i, \delta_i, \varepsilon_i, \phi_i, \tau_i\}$, the ODEs for the corresponding $P_i(t)$ and $N_i(t)$ are solved numerically. The parameter values tested for each species score are given in *SI Appendix*, Table S4. The resultant upper and lower layer components of the neuronal output, labeled U_i and L_i, respectively, are calculated as follows:

$$U_i = \int_0^1 \frac{dN_i(t)}{dt}(u(t+\tau_i))dt; \quad L_i = \int_0^1 \frac{dN_i(t)}{dt}(1-u(t+\tau_i))dt.$$

To evaluate how well U_i, L_i, and $P_i(1)$, as arising from the choice of parameters m_i, reproduce the target values for the given cortex score, the "error"

$$E_i = |P_i(1)| + |U_i - U_T| + |L_i - L_T|$$

is calculated. Here U_T and L_T are the upper and lower layer neuronal output targets for the given species (as in Fig. 1*A*) and $P_i(1)$ is the relative size of the precursor pool at the end of neurogenesis. The particular set of parameters m_i which minimizes E_i for a given cortex score is denoted $m_* = \{\alpha_*, \beta_*, \gamma_*, \delta_*, \varepsilon_*, \phi_*, \tau_*\}$. We label the corresponding upper and lower layer neuronal output as U_* and L_*, respectively. We checked over 5×10^5 parameter sets for each cortex score.

Modeling the Effects of Spatial Gradients in Neurogenesis. Viewing the parameters m_* identified above as applying to the "average" location in cortex, the effects of progressing the corresponding parameter functions, from their starting values through to their end values, more quickly in anterior cortex and more slowly in posterior cortex may be examined (see *SI Appendix*, section S7 for the mathematical formulation). At the "average cortical location" the parameter functions are unaffected by the scaling. At the extremities of the spatial axis parameter functions are progressed 10% faster and slower, respectively, than at the average location. Solving a separate pair of differential equaions for each spatially indexed $P_x(t)$ and $N_x(t)$ produces location-dependent upper and lower layer outputs U_x and L_x (Fig. 3).

ACKNOWLEDGMENTS. We thank Richard Darlington, Veit Elser, Joel Nishimura, Tim Novikoff, Olaf Sporns, and Steven Strogatz for helpful discussions. This work was supported by National Science Foundation (NSF)/Conselho Nacional de Desenvolvimento Cientifico e Tecnologico Grant 910149/96-99 to Luis Carlos de Lima Silveira, NSF Grant IBN-0138113 (to B.L.F.), Eunice Kennedy Shriver National Institute of Child Health and Human Development Fellowship F32HD067011 (to C.J.C.), a National University of Ireland Traveling Studentship (to D.J.C.), and NSF Grant CCF-0835706 to Steven Strogatz.

1. Yopak KE, et al. (2010) A conserved pattern of brain scaling from sharks to primates. *Proc Natl Acad Sci USA* 107(29):12946–12951.
2. Finlay BL, Hinz F, Darlington RB (2011) Mapping behavioural evolution onto brain evolution: The strategic roles of conserved organization in individuals and species. *Philos Trans R Soc Lond B Biol Sci* 366(1574):2111–2123.
3. Charvet CJ, Darlington RB, Finlay BL (2013) Variation in human brains may facilitate evolutionary change toward a limited range of phenotypes. *Brain Behav Evol* 81(2):74–85.
4. Finlay BL, Darlington RB (1995) Linked regularities in the development and evolution of mammalian brains. *Science* 268(5217):1578–1584.
5. Takahashi T, Nowakowski RS, Caviness VS, Jr (1996) The leaving or Q fraction of the murine cerebral proliferative epithelium: A general model of neocortical neuronogenesis. *J Neurosci* 16(19):6183–6196.
6. Takahashi T, Nowakowski RS, Caviness VS, Jr (1997) The mathematics of neocortical neuronogenesis. *Dev Neurosci* 19(1):17–22.
7. Nowakowski RS, Caviness VS, Takahashi T, Hayes NL (2002) *Cortical Development*, ed Hohmann C (Springer, Berlin), pp 1–25.
8. Caviness VS, Jr, et al. (2003) Cell output, cell cycle duration and neuronal specification: A model of integrated mechanisms of the neocortical proliferative process. *Cereb Cortex* 13(6):592–598.
9. Gohlke JM, Griffith WC, Bartell SM, Lewandowski TA, Faustman EM (2002) A computational model for neocortical neuronogenesis predicts ethanol-induced neocortical neuron number deficits. *Dev Neurosci* 24(6):467–477.
10. Gohlke JM, Griffith WC, Faustman EM (2007) Computational models of neocortical neuronogenesis and programmed cell death in the developing mouse, monkey, and human. *Cereb Cortex* 17(10):2433–2442.
11. McConnell SK (1995) Constructing the cerebral cortex: Neurogenesis and fate determination. *Neuron* 15(4):761–768.
12. Betizeau M, et al. (2013) Precursor diversity and complexity of lineage relationships in the outer subventricular zone of the primate. *Neuron* 80(2):442–457.
13. Bayer SA, Altman J (1991) *Neocortical Development* (Raven, New York).
14. Rakic P (1982) Early developmental events: Cell lineages, acquisition of neuronal positions, and areal and laminar development. *Neurosci Res Program Bull* 20(4):439–451.
15. Price DJ, et al. (2006) The development of cortical connections. *Eur J Neurosci* 23(4):910–920.
16. Dehay C, Kennedy H (2007) Cell-cycle control and cortical development. *Nat Rev Neurosci* 8(6):438–450.
17. Yamamori T (2011) Selective gene expression in regions of primate neocortex: Implications for cortical specialization. *Prog Neurobiol* 94(3):201–222.
18. Haydar TF, Nowakowski RS, Yarowsky PJ, Krueger BK (2000) Role of founder cell deficit and delayed neuronogenesis in microencephaly of the trisomy 16 mouse. *J Neurosci* 20(11):4156–4164.
19. Clancy B, Darlington RB, Finlay BL (2001) Translating developmental time across mammalian species. *Neuroscience* 105(1):7–17.
20. Charvet CJ, Cahalane DJ, Finlay BL (2013) Systematic, cross-cortex variation in neuron numbers in rodents and primates. *Cereb Cortex*, 10.1093/cercor/bht214.
21. Christensen JR, et al. (2007) Neocortical and hippocampal neuron and glial cell numbers in the rhesus monkey. *Anat Rec (Hoboken)* 290(3):330–340.
22. Roth G, Dicke U (2005) Evolution of the brain and intelligence. *Trends Cogn Sci* 9(5):250–257.
23. Korbo L, et al. (1990) An efficient method for estimating the total number of neurons in rat brain cortex. *J Neurosci Methods* 31(2):93–100.
24. Hutsler JJ, Lee D-G, Porter KK (2005) Comparative analysis of cortical layering and supragranular layer enlargement in rodent carnivore and primate species. *Brain Res* 1052(1):71–81.
25. Takahashi T, Nowakowski RS, Caviness VS, Jr (1995) The cell cycle of the pseudostratified ventricular epithelium of the embryonic murine cerebral wall. *J Neurosci* 15(9):6046–6057.
26. Miller MW, Kuhn PE (1995) Cell cycle kinetics in fetal rat cerebral cortex: Effects of prenatal treatment with ethanol assessed by a cumulative labeling technique with flow cytometry. *Alcohol Clin Exp Res* 19(1):233–237.
27. Kornack DR, Rakic P (1998) Changes in cell-cycle kinetics during the development and evolution of primate neocortex. *Proc Natl Acad Sci USA* 95(3):1242–1246.
28. Reillo I, Borrell V (2012) Germinal zones in the developing cerebral cortex of ferret: Ontogeny, cell cycle kinetics, and diversity of progenitors. *Cereb Cortex* 22(9):2039–2054.
29. Lukaszewicz A, et al. (2005) G1 phase regulation, area-specific cell cycle control, and cytoarchitectonics in the primate cortex. *Neuron* 47(3):353–364.
30. Cahalane DJ, Charvet CJ, Finlay BL (2012) Systematic, balancing gradients in neuron density and number across the primate isocortex. *Front Neuroanat* 6:28.
31. Collins CE, Airey DC, Young NA, Leitch DB, Kaas JH (2010) Neuron densities vary across and within cortical areas in primates. *Proc Natl Acad Sci USA* 107(36):15927–15932.
32. Luskin MB, Shatz CJ (1985) Neurogenesis of the cat's primary visual cortex. *J Comp Neurol* 242(4):611–631.
33. Jackson CA, Peduzzi JD, Hickey TL (1989) Visual cortex development in the ferret. I. Genesis and migration of visual cortical neurons. *J Neurosci* 9(4):1242–1253.
34. Miyama S, Takahashi T, Nowakowski RS, Caviness VS, Jr (1997) A gradient in the duration of the G1 phase in the murine neocortical proliferative epithelium. *Cereb Cortex* 7(7):678–689.
35. Rakic P (2002) Neurogenesis in adult primate neocortex: An evaluation of the evidence. *Nat Rev Neurosci* 3(1):65–71.
36. Smart IHM, Dehay C, Giroud P, Berland M, Kennedy H (2002) Unique morphological features of the proliferative zones and postmitotic compartments of the neural epithelium giving rise to striate and extrastriate cortex in the monkey. *Cereb Cortex* 12(1):37–53.
37. Finlay BL, Slattery M (1983) Local differences in the amount of early cell death in neocortex predict adult local specializations. *Science* 219(4590):1349–1351.
38. Van Essen DC, Anderson CH, Felleman DJ (1992) Information processing in the primate visual system: An integrated systems perspective. *Science* 255(5043):419–423.
39. Modha DS, Singh R (2010) Network architecture of the long-distance pathways in the macaque brain. *Proc Natl Acad Sci USA* 107(30):13485–13490.
40. Markov NT, et al. (2013) Cortical high-density counterstream architectures. *Science* 342(6158):1238406–1238406.
41. Harriger L, van den Heuvel MP, Sporns O (2012) Rich club organization of macaque cerebral cortex and its role in network communication. *PLoS ONE* 7(9):e46497.
42. Burek MJ, Oppenheim RW (1996) Programmed cell death in the developing nervous system. *Brain Pathol* 6(4):427–446.
43. Underwood E (2013) Mysteries of development. Why do so many neurons commit suicide during brain development? *Science* 340(6137):1157–1158.
44. Thomaidou D, Mione MC, Cavanagh JF, Parnavelas JG (1997) Apoptosis and its relation to the cell cycle in the developing cerebral cortex. *J Neurosci* 17(3):1075–1085.